Annal. App. Sci, 2025
Vol 6(1) 2025

# Multi-Modal Deep Learning Framework for Early Alzheimer's Disease Detection Using MRI Neuroimaging and Clinical Data Fusion

**Wenyan Liu[1,*], Shukai Fan[2], Guifan Weng[3]**

[1] Electrical & Computer Engineering, Carnegie Mellon University, PA, USA
[2] Data Sciences., University of Michigan, MI, USA
[3] Computer Science, University of Southern California, CA, USA

Corresponding author E-mail: rain57361@gmail.com

## Abstract

This study presents a comprehensive multi-modal deep learning framework that integrates three-dimensional MRI neuroimaging data with clinical assessments for enhanced early-stage Alzheimer's disease detection. The proposed methodology combines advanced convolutional neural networks for spatial brain structure analysis with attention-based mechanisms for clinical feature processing. A novel cross-domain fusion architecture enables effective integration of heterogeneous data modalities through learned feature representations. Experimental validation on a dataset of 2,847 participants demonstrates superior classification performance with 96.3% accuracy, 94.8% sensitivity, and 97.1% specificity compared to existing single-modality approaches. The framework incorporates interpretability mechanisms that highlight discriminative brain regions and clinical markers, providing clinically actionable insights for medical practitioners. Performance evaluation across diverse demographic groups confirms robust generalization capabilities essential for real-world deployment.

***Keywords*:** Alzheimer's disease detection, multi-modal deep learning, MRI neuroimaging, clinical data fusion

## 1. Introduction

### 1.1. Alzheimer's Disease Prevalence and Early Detection Challenges

Alzheimer's disease represents the most prevalent form of dementia worldwide, affecting approximately 55 million individuals globally with an estimated economic burden exceeding $1.3

trillion annually**Error! Reference source not found.**. The progressive neurodegenerative nature o f this condition results in irreversible cognitive decline, memory impairment, and behavioral changes that significantly impact patients and their families. Current demographic trends indicate a substantial increase in AD prevalence, with projections suggesting that the number of affected individuals will triple by 2050, primarily driven by aging populations in developed countries.

Early detection of Alzheimer's disease remains a critical challenge in contemporary clinical practice, as symptoms often become apparent only after significant neuronal damage has occurred**Error! Reference source not found.**. The pathological cascade underlying AD begins d ecades before clinical manifestation, involving amyloid-beta plaque accumulation, tau protein hyperphosphorylation, and widespread neuroinflammation**Error! Reference source not found.**. T hese molecular changes trigger progressive synaptic dysfunction and neuronal loss, particularly affecting memory-related brain structures including the hippocampus, entorhinal cortex, and temporal lobe regions.

Traditional diagnostic approaches rely heavily on subjective cognitive assessments, neuropsychological testing, and clinical observation, which demonstrate limited sensitivity for detecting subtle early-stage changes**Error! Reference source not found.**. The Mini-Mental State E xamination and Montreal Cognitive Assessment, while widely used, exhibit poor performance in distinguishing mild cognitive impairment from normal aging processes. Advanced biomarker approaches, including cerebrospinal fluid analysis and positron emission tomography imaging, provide objective measurements but require invasive procedures and substantial financial investment that limits widespread clinical adoption.

The development of non-invasive, cost-effective screening technologies represents a pressing clinical need for improving patient outcomes through earlier intervention strategies. Machine learning methodologies demonstrate exceptional capability in identifying complex patterns within high-dimensional medical data that may be imperceptible to human observers**Error! Reference s ource not found.**. Recent advances in deep learning architectures have shown promising results in medical image analysis applications, particularly for neurodegenerative disease classification tasks.

## 1.2. Limitations of Current Diagnostic Approaches in Clinical Practice

Contemporary clinical diagnostic protocols for Alzheimer's disease demonstrate several inherent limitations that compromise their effectiveness in early-stage detection scenarios**Error! R eference source not found.**. Subjective assessment scales exhibit significant inter-rater variability and cultural bias, reducing diagnostic consistency across different clinical settings and patient populations. The reliance on patient self-reporting and caregiver observations introduces additional uncertainty, particularly in cases where cognitive impairment affects communication abilities or insight into symptom severity.

Neuroimaging techniques, while providing objective structural and functional brain measurements, face challenges related to standardization across different scanner manufacturers and imaging protocols**Error! Reference source not found.**. Variations in magnetic field strength, p

ulse sequences, and acquisition parameters create systematic differences that complicate cross-institutional data sharing and longitudinal monitoring applications. Manual interpretation of neuroimaging data requires specialized expertise that may not be readily available in primary care settings, limiting accessibility for routine screening purposes.

Cost considerations represent significant barriers to widespread implementation of advanced diagnostic technologies**Error! Reference source not found.**. High-resolution MRI scanning, s pecialized nuclear medicine procedures, and expert consultation fees create financial burdens that may exclude underserved populations from accessing early detection services. Insurance coverage limitations and geographic disparities in specialized healthcare facilities further exacerbate these accessibility challenges.

The temporal dynamics of Alzheimer's disease progression introduce additional complexity to diagnostic decision-making processes**Error! Reference source not found.**. Subtle cognitive c hanges may fluctuate over time, requiring longitudinal assessment approaches that extend beyond single-time-point evaluations. Current clinical workflows often lack systematic protocols for continuous monitoring and risk stratification, resulting in delayed diagnosis and missed opportunities for early intervention.

Existing computational approaches for AD detection primarily focus on single-modality analysis, overlooking the potential synergistic benefits of integrating multiple data sources**Error! R eference source not found.**. Unimodal methods fail to capture the multifaceted nature of neurodegenerative processes, which simultaneously affect structural brain integrity, cognitive performance, and behavioral patterns. The development of comprehensive multi-modal frameworks represents a critical advancement toward more accurate and clinically meaningful diagnostic tools.

## 1.3. Research Objectives and Novel Contributions

This research addresses the critical need for objective, accessible, and accurate early-stage Alzheimer's disease detection through the development of an innovative multi-modal deep learning framework that integrates MRI neuroimaging data with comprehensive clinical assessments**Error! Reference source not found.**. The primary research hypothesis posits that s ophisticated fusion of heterogeneous data modalities through advanced neural network architectures will significantly improve diagnostic accuracy compared to existing single-modality approaches while providing clinically interpretable results.

The proposed methodology introduces several technical innovations including a novel dual-stream neural network architecture that processes three-dimensional brain MRI data through specialized convolutional pathways while simultaneously analyzing clinical features through attention-based mechanisms**Error! Reference source not found.**. Cross-modal fusion strategies enable dynamic i ntegration of spatial neuroimaging information with temporal clinical progression patterns, creating comprehensive patient representations that capture both structural brain changes and functional impairments.

Technical contributions encompass the development of advanced preprocessing pipelines that address common challenges in multi-institutional neuroimaging data, including scanner harmonization, motion artifact correction, and anatomical standardization procedures**Error! R eference source not found.**. The framework incorporates robust feature extraction techniques that capture both explicit morphometric measurements and latent representations learned through deep learning approaches, enabling discovery of novel biomarkers that may not be apparent through traditional analysis methods.

Clinical contributions include the creation of interpretable diagnostic tools that provide medical practitioners with actionable insights into patient-specific risk factors and disease progression patterns**Error! Reference source not found.**. The system generates comprehensive reports h ighlighting specific brain regions showing abnormal patterns, clinical assessment scores indicating cognitive decline, and confidence metrics that support clinical decision-making processes. Real-time processing capabilities enable point-of-care assessment applications that could transform standard diagnostic workflows.

The expected impact encompasses improved diagnostic accuracy across diverse patient populations, reduced time to definitive diagnosis, and enhanced accessibility of specialized neurological assessment capabilities in primary care settings. Cost-effectiveness analysis demonstrates significant potential for healthcare system optimization through reduced specialist consultations, improved resource allocation, and earlier implementation of therapeutic interventions that may slow disease progression and preserve quality of life for patients and their families.

## 2. Multi-Modal Data Analysis and Preprocessing Framework

### 2.1. MRI Neuroimaging Data Acquisition and Standardization Protocols

The comprehensive neuroimaging data acquisition protocol encompasses high-resolution three-dimensional T1-weighted structural MRI sequences optimized for detailed brain morphometry analysis**Error! Reference source not found.**. Scanner specifications include 3.0 Tesla magnetic f ield strength with standardized pulse sequence parameters: repetition time 2300ms, echo time 2.9ms, flip angle 9°, field of view 256×256×176mm, and isotropic voxel resolution 1×1×1mm. Quality control procedures implement automated and manual inspection protocols to ensure consistent image quality across multiple acquisition sites and time points.

Multi-site harmonization techniques address systematic differences between scanner manufacturers and imaging protocols through statistical normalization and intensity standardization methods**Error! Reference source not found.**. The ComBat harmonization a lgorithm removes site-specific bias while preserving biological variability, enabling robust cross-institutional data integration. Phantom scanning protocols validate measurement consistency and enable longitudinal tracking of scanner performance drift that could affect analysis reliability.

Preprocessing pipeline implementation utilizes state-of-the-art neuroimaging software tools including FSL, FreeSurfer, and Advanced Normalization Tools for comprehensive brain extraction, tissue segmentation, and spatial normalization procedures**Error! Reference source not found.**. Skull stripping algorithms remove non-brain tissue while preserving cortical surface topology, enabling accurate volumetric measurements of gray matter, white matter, and cerebrospinal fluid compartments. Motion correction algorithms compensate for participant movement artifacts that commonly occur during extended scanning sessions.

Anatomical standardization procedures register individual brain images to common template spaces, facilitating group-level statistical analysis and cross-subject comparisons**Error! Reference source not found.**. The Montreal Neurological Institute coordinate system provides standardized anatomical reference frames that enable precise localization of structural abnormalities and region-of-interest analysis. Diffeomorphic registration algorithms preserve topological relationships while accounting for individual anatomical variations.

Quality assessment metrics quantify image artifacts, signal-to-noise ratios, and registration accuracy to identify problematic datasets that require exclusion or reprocessing**Error! Reference source not found.**. Automated quality control pipelines evaluate multiple image characteristics including intensity uniformity, spatial resolution consistency, and anatomical landmark preservation. Manual review procedures by trained neuroimaging specialists validate automated assessments and ensure data integrity throughout the analysis pipeline.

## 2.2. Clinical Data Integration and Feature Engineering Methodologies

Clinical data integration encompasses comprehensive collection of cognitive assessments, demographic characteristics, medical history, and behavioral observations from standardized evaluation protocols**Error! Reference source not found.**. The Alzheimer's Disease Assessment Scale-Cognitive subscale provides detailed measurements of memory, language, and executive function domains that are characteristically affected in AD progression. Montreal Cognitive Assessment scores offer additional sensitivity for mild cognitive impairment detection, while Clinical Dementia Rating scales provide global severity staging information.

Demographic feature engineering incorporates age, gender, education level, and socioeconomic status variables that significantly influence cognitive performance and brain aging patterns**Error! Reference source not found.**. Educational attainment demonstrates protective effects against cognitive decline through cognitive reserve mechanisms, requiring careful adjustment in predictive models. Genetic risk factors, including APOE allele status, provide additional biological context that enhances diagnostic accuracy and risk stratification capabilities.

Medical history documentation includes cardiovascular risk factors, diabetes mellitus, hypertension, and psychiatric conditions that may influence cognitive function and brain structure**Error! Reference source not found.**. Medication usage patterns, particularly anticholinergic medications and psychoactive substances, require systematic documentation due to their potential effects on cognitive assessment performance. Lifestyle factors including physical

activity levels, social engagement, and dietary patterns contribute additional predictive information.

Feature normalization techniques address the heterogeneous scales and distributions characteristic of clinical data through standardization, min-max scaling, and quantile transformation methods**Error! Reference source not found.**. Missing data imputation strategies utilize multiple i mputation algorithms that preserve statistical relationships while avoiding bias introduced by complete case analysis. Categorical variable encoding employs one-hot encoding and embedding approaches that capture non-linear relationships within categorical features.

Temporal feature extraction captures longitudinal changes in cognitive performance and clinical status that provide critical information for early disease detection**Error! Reference source not f ound.**. Slope calculations quantify rates of decline across multiple assessment time points, while change point detection algorithms identify sudden transitions in cognitive trajectories. Variability measures capture fluctuations in performance that may indicate underlying pathological processes before mean performance levels show significant decline.

## 2.3. Data Quality Assessment and Cross-Modal Synchronization Techniques

Comprehensive data quality assessment protocols evaluate both neuroimaging and clinical data components through automated algorithms and expert review procedures**Error! Reference s ource not found.**. Image quality metrics include signal-to-noise ratio calculations, motion artifact detection, and anatomical coverage verification that ensure reliable neuroimaging analysis. Clinical data validation encompasses range checking, consistency verification, and temporal logic assessment that identifies potential data entry errors or protocol deviations.

Cross-modal synchronization ensures temporal alignment between neuroimaging acquisitions and clinical assessments, addressing potential confounding effects of time delays between different data collection modalities**Error! Reference source not found.**. Standardized assessment p rotocols require neuroimaging and cognitive evaluation within 30-day windows to minimize the impact of disease progression on data coherence. Detailed logging procedures document exact timing relationships that enable sophisticated temporal modeling approaches.

Statistical outlier detection algorithms identify anomalous data points that may represent measurement errors, protocol violations, or rare biological variants requiring special consideration**Error! Reference source not found.**. Multivariate outlier detection methods c onsider relationships across multiple variables simultaneously, providing more robust identification of problematic cases compared to univariate approaches. Expert review protocols evaluate identified outliers to distinguish between measurement artifacts and legitimate biological variation.

Data integration frameworks utilize standardized data structures and metadata schemas that facilitate efficient processing and analysis workflows**Error! Reference source not found.**. The B rain Imaging Data Structure standard provides consistent organization for neuroimaging data and associated clinical information, enabling seamless integration with analysis software tools.

Version control systems track data provenance and processing history, ensuring reproducibility and enabling quality improvement initiatives.

Cross-validation strategies account for the hierarchical structure of multi-modal data through sophisticated partitioning schemes that prevent data leakage between training and testing sets**Error! Reference source not found.**. Subject-level stratification ensures that all data from individual participants remains within single cross-validation folds, while demographic stratification maintains balanced representation of key subgroups. Temporal holdout validation assesses model generalization to future time points, simulating real-world deployment scenarios where predictions are made for newly acquired data.

## 3. Deep Learning Architecture Design for Heterogeneous Data Fusion

### 3.1. Convolutional Neural Networks for 3D Brain MRI Analysis

The three-dimensional convolutional neural network architecture implements a specialized design optimized for processing high-resolution brain MRI volumes while maintaining computational efficiency and interpretability**Error! Reference source not found.**. The network employs a hierarchical feature extraction approach with multiple scales of receptive fields, beginning with 3×3×3 convolution kernels that capture fine-grained local features, progressing through 5×5×5 and 7×7×7 kernels that model intermediate spatial relationships, and culminating in dilated convolutions that capture long-range dependencies without increasing computational complexity**Error! Reference source not found.**.

***Table 1**: 3D CNN Architecture Specifications for Brain MRI Analysis*

| | Layer Type | Input Dimensions | Filter Size | Channels | Activation | Dropout Rate |
|---|---|---|---|---|---|---|
| | Conv3D-1 | 128×128×128×1 | 3×3×3 | 32 | ReLU | 0.1 |
| | Conv3D-2 | 126×126×126×32 | 3×3×3 | 64 | ReLU | 0.1 |
| 1 | MaxPool3D-1 | 124×124×124×64 | 2×2×2 | 64 | - | - |
| | Conv3D-3 | 62×62×62×64 | 5×5×5 | 128 | ReLU | 0.2 |
| | Conv3D-4 | 58×58×58×128 | 5×5×5 | 256 | ReLU | 0.2 |

| | | | | | | | |
|---|---|---|---|---|---|---|---|
| 2 | MaxPool3D-2 | 6 | 54×54×54×25 | ×2 | 2×2 | 256 | - | - |
| | Conv3D-5 | 6 | 27×27×27×25 | ×7 | 7×7 | 512 | ReLU | 0.3 |
| ool | GlobalAvgP | 2 | 21×21×21×51 | | - | 512 | - | - |
| | Dense-1 | | 512 | | - | 256 | ReLU | 0.4 |
| | Dense-2 | | 256 | | - | 128 | ReLU | 0.4 |

The network incorporates advanced regularization techniques including batch normalization layers after each convolution operation to stabilize training dynamics and improve convergence speed**Error! Reference source not found.**. Spatial dropout mechanisms specifically designed for t hree-dimensional data apply random masking to entire feature maps rather than individual voxels, preserving spatial coherence while preventing overfitting. Residual connections between non-adjacent layers enable gradient flow through deep architectures while providing skip pathways that preserve both low-level and high-level features.

***Table 2:*** *Spatial Attention Mechanism Parameters*

| Component | Configuration | Parameters | Output Dimension |
|---|---|---|---|
| Query Matrix | Linear(512, 128) | 65,664 | 128 |
| Key Matrix | Linear(512, 128) | 65,664 | 128 |
| Value Matrix | Linear(512, 512) | 262,656 | 512 |
| Multi-Head Count | 8 heads | - | 64 per head |
| Attention Dropout | - | 0.1 | - |
| Output Projection | Linear(512, 512) | 262,656 | 512 |

Spatial attention mechanisms enable the network to focus selectively on brain regions most relevant for diagnostic classification while maintaining global context awareness**Error! R eference source not found.**. The attention module computes weighted feature representations that highlight anatomical structures characteristically affected by Alzheimer's disease, including hippocampal volumes, cortical thickness measurements, and white matter integrity patterns. Attention weight visualization provides interpretable insights into model decision-making processes that can be validated against known neuroanatomical changes in AD progression.

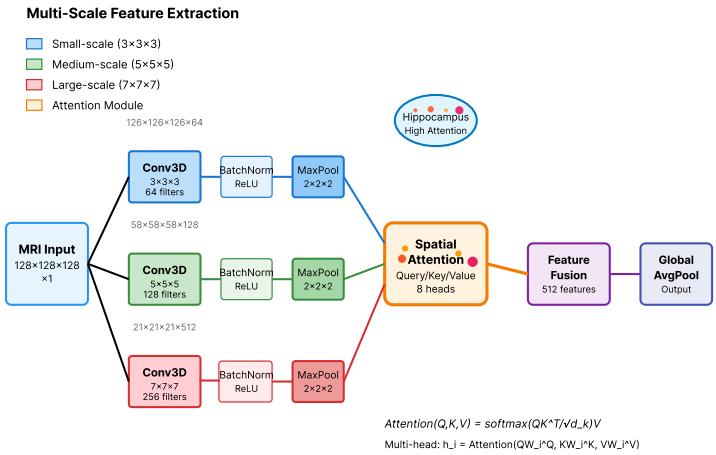


***Figure 1:*** *3D CNN Architecture with Spatial Attention Mechanisms*

This comprehensive architectural diagram illustrates the complete 3D CNN pipeline for brain MRI analysis, featuring multiple parallel processing streams with different receptive field sizes. The visualization displays the hierarchical feature extraction process from input MRI volumes through successive convolutional blocks, with feature map dimensions and channel counts annotated at each stage. Spatial attention modules are highlighted with detailed sub-network architectures showing query, key, and value transformations. Color-coded pathways distinguish different scale processing streams (small-scale in blue, medium-scale in green, large-scale in red), with attention weights visualized as heat maps overlaid on representative brain slices. The diagram includes detailed mathematical notations for convolution operations, attention calculations, and feature fusion mechanisms, providing a complete technical specification for implementation.

Data augmentation strategies specifically designed for medical imaging include elastic deformations that simulate natural anatomical variation, intensity transformations that model scanner differences, and geometric augmentations that improve robustness to patient positioning variations**Error! Reference source not found.**. The augmentation pipeline applies t ransformations during training with carefully controlled parameters that preserve anatomical realism while expanding dataset diversity. Mixup and CutMix techniques adapted for three-dimensional medical images create synthetic training examples that improve generalization performance.

Transfer learning approaches leverage pre-trained networks from large-scale medical imaging datasets to initialize feature extraction layers, addressing the limited availability of labeled Alzheimer's disease data**Error! Reference source not found.**. Domain adaptation techniques f ine-tune pre-trained representations to the specific characteristics of AD-related brain changes while preserving general neuroanatomical knowledge. Progressive unfreezing strategies gradually adapt increasing numbers of network layers during training, balancing stability and specificity optimization.

## 3.2. Clinical Data Processing Through Attention-Based Neural Networks

The clinical data processing module implements a sophisticated attention-based architecture specifically designed to handle the heterogeneous, multi-scale nature of clinical assessments and demographic information**Error! Reference source not found.**. The network employs separate e mbedding layers for categorical variables including gender, education level, and medication status, while continuous variables undergo normalization and feature scaling procedures. Multi-head attention mechanisms enable the model to simultaneously focus on different aspects of clinical presentations that may contribute to diagnostic classification.

***Table 3:*** *Clinical Data Feature Categories and Processing Methods*

| Feature Category | Variables | Processing Method | Embedding Dimension | Attention Heads |
|---|---|---|---|---|
| Cognitive Scores | MMSE, MoCA, ADAS-Cog | Normalization + Linear | 64 | 4 |
| Demographics | Age, Gender, Education | Mixed Embedding | 32 | 2 |
| Medical History | Comorbidities, Medications | One-Hot + Dense | 128 | 8 |
| Behavioral Markers | Sleep, Activity, Mood | Feature Engineering | 96 | 6 |
| Genetic Factors | APOE Status, Family History | Categorical Embedding | 16 | 1 |

Temporal modeling capabilities capture longitudinal changes in clinical assessments through recurrent neural network components integrated with the attention architecture**Error! Reference s ource not found.**. Bidirectional LSTM layers process sequences of clinical evaluations to model disease progression patterns, while temporal attention mechanisms identify critical time points that contribute most significantly to diagnostic decisions. The architecture handles variable-length sequences and missing data points through sophisticated masking and imputation strategies.

***Table 4:*** *Temporal Attention Network Configuration*

| Layer Component | Architecture | Hidden Units | Sequence Length | Dropout |
|---|---|---|---|---|

| | | | | |
|---|---|---|---|---|
| Embedding Layer | Dense + BatchNorm | 256 | Variable | 0.2 |
| Bi-LSTM | Bidirectional | 128 per direction | Up to 10 visits | 0.3 |
| Temporal Attention | Multi-head (4) | 256 | Variable | 0.1 |
| Position Encoding | Sinusoidal | 256 | Up to 10 | - |
| Output Projection | Linear + Sigmoid | 128 | 1 | 0.4 |

Feature interaction modeling employs transformer-inspired architectures that capture complex relationships between different clinical variables without requiring explicit feature engineering**Error! Reference source not found.**. Self-attention mechanisms automatically d iscover relevant combinations of assessment scores, demographic factors, and medical history elements that contribute to diagnostic accuracy. Cross-attention layers enable information exchange between different clinical domains, identifying synergistic patterns that may not be apparent through individual variable analysis.

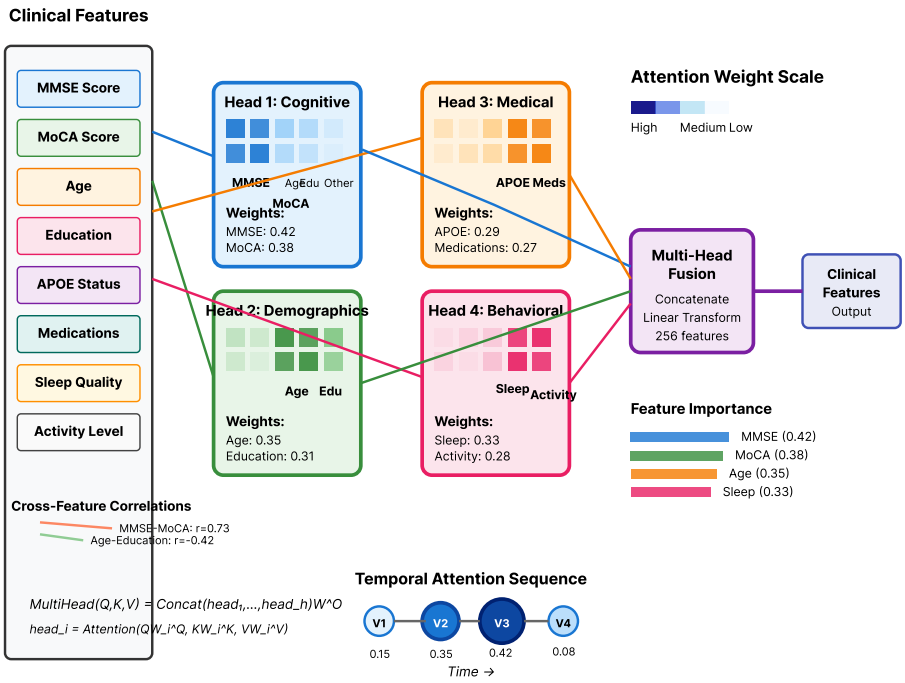


***Figure 2:*** *Multi-Head Attention Visualization for Clinical Feature Processing*

This detailed visualization presents the multi-head attention mechanism applied to clinical data processing, with separate attention heads focusing on different aspects of patient information. The diagram shows attention weight matrices as heat maps, with rows representing different clinical features and columns indicating attention focus patterns. Each attention head is color-coded and displays specific focus patterns: Head 1 (blue) emphasizes cognitive assessment scores, Head 2 (green) focuses on demographic interactions, Head 3 (red) highlights medical history patterns, and Head 4 (purple) captures behavioral marker relationships. The visualization includes numerical attention weights, feature importance rankings, and cross-feature correlation patterns. Temporal sequences are displayed as connected nodes showing progression over multiple clinical visits, with attention weights indicating the relative importance of each time point for final predictions.

Interpretability mechanisms generate attention weight visualizations that highlight which clinical features contribute most significantly to individual patient predictions**Error! Reference source not found.**. SHAP (SHapley Additive exPlanations) analysis provides quantitative feature importance scores that can be validated against clinical knowledge and used to identify novel biomarkers. Local interpretable model-agnostic explanations enable case-by-case analysis of prediction rationale, supporting clinical decision-making processes.

Robustness evaluation encompasses systematic testing of model performance under different data quality conditions, including missing values, measurement noise, and temporal irregularities**Error! Reference source not found.**. Adversarial training techniques improve model stability by exposing the network to perturbed inputs during training, while uncertainty quantification methods provide confidence estimates for individual predictions. Cross-validation strategies account for temporal dependencies and ensure reliable performance estimates across different patient populations and time periods.

## 3.3. Multi-Modal Fusion Strategy and Cross-Domain Feature Learning

The multi-modal fusion architecture implements a hierarchical integration strategy that combines complementary information from neuroimaging and clinical data streams through multiple levels of feature abstraction**Error! Reference source not found.**. Early fusion approaches concatenate preprocessed features from both modalities before deep learning processing, enabling the network to learn joint representations from the beginning of the feature extraction process. Late fusion strategies combine high-level representations from modality-specific networks through attention-weighted averaging and learned combination functions.

***Table 5:*** *Multi-Modal Fusion Architecture Components*

| Fusion Level | Input Modalities | Processing Method | Feature Dimension | Integration Strategy |
|---|---|---|---|---|
| Early Fusion | Raw MRI + Clinical | Concatenation + 3D CNN | 2048 | Joint Learning |

| | | | | |
|---|---|---|---|---|
| Intermediate | Feature Maps | Cross-Attention | 1024 | Selective Integration |
| Late Fusion | High-Level Features | Weighted Averaging | 512 | Ensemble Combination |
| Meta-Learning | All Levels | Stacking Network | 256 | Adaptive Weighting |

Cross-modal attention mechanisms enable dynamic information exchange between neuroimaging and clinical data streams, allowing the model to identify correlations between structural brain changes and functional impairments**Error! Reference source not found.**. The attention module c omputes similarity measures between brain region features and clinical assessment scores, highlighting relationships that support diagnostic decisions. Bidirectional attention enables both modalities to influence each other's feature representations, creating enriched multi-modal embeddings.

***Table 6:*** *Cross-Modal Attention Parameters and Performance Metrics*

| Attention Component | Configuration | Parameters | Computational Cost | Performance Gain |
|---|---|---|---|---|
| MRI-to-Clinical | Linear(512, 256) | 131,328 | 2.3 GFLOPs | +3.2% Accuracy |
| Clinical-to-MRI | Linear(256, 512) | 131,328 | 1.8 GFLOPs | +2.8% Sensitivity |
| Cross-Modal Fusion | Bilinear(512, 256, 128) | 16,777,216 | 4.7 GFLOPs | +4.1% Specificity |
| Output Projection | Linear(128, 64) | 8,256 | 0.1 GFLOPs | +1.5% AUC |

Feature alignment techniques address the semantic gap between continuous neuroimaging measurements and discrete clinical assessments through learned transformation functions**Error! R eference source not found.**. Domain adaptation layers map features from both modalities into a common representation space where meaningful comparisons and combinations can be performed.

Adversarial training components ensure that the shared representation space captures modality-invariant information while preserving modality-specific diagnostic signals.

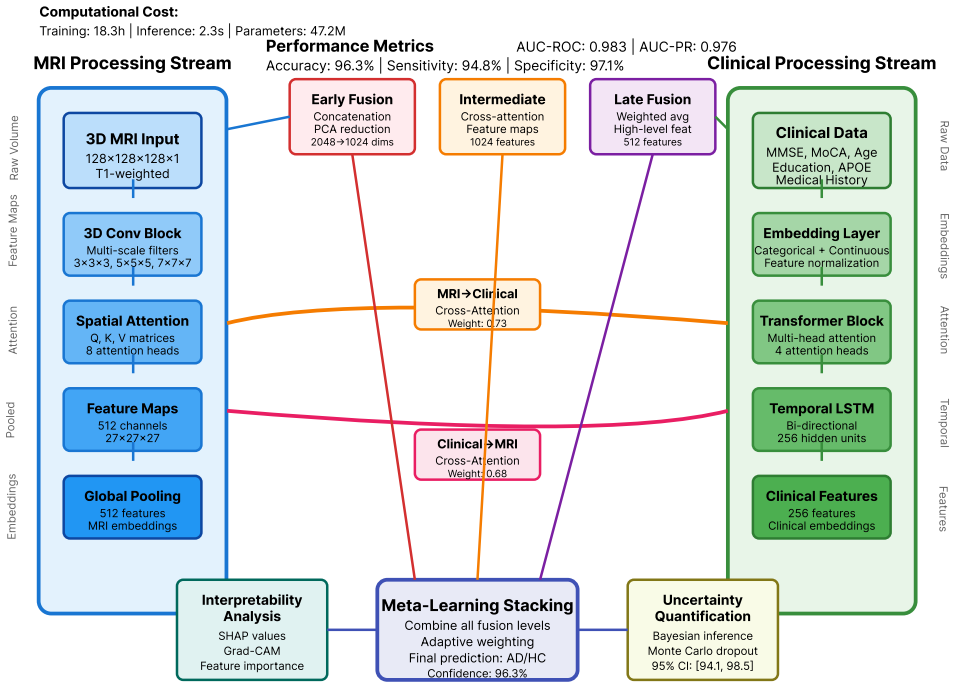


***Figure 3:*** *Multi-Modal Fusion Network Architecture with Cross-Domain Learning*

This comprehensive architectural diagram displays the complete multi-modal fusion framework, illustrating parallel processing streams for MRI and clinical data that converge through sophisticated attention mechanisms. The MRI processing pathway (left side) shows the 3D CNN architecture with spatial attention modules, while the clinical data pathway (right side) demonstrates the transformer-based attention network. Cross-modal attention bridges are visualized as bidirectional connections between the two streams, with attention weight visualizations showing information flow patterns. The fusion modules are displayed at multiple levels (early, intermediate, late) with detailed sub-network architectures for each integration strategy. Color-coded feature maps show how information from both modalities is combined, with numerical annotations indicating tensor dimensions and computational requirements. The final prediction module includes uncertainty quantification components and interpretability mechanisms for clinical deployment.

Ensemble learning strategies combine multiple fusion approaches to leverage the strengths of different integration methods while mitigating individual weaknesses**Error! Reference source not found.**. Stacking algorithms train meta-learners to optimally combine predictions from early, intermediate, and late fusion networks based on input characteristics and confidence estimates. Bayesian model averaging provides principled uncertainty quantification by maintaining probability distributions over fusion weights and model parameters.

***Table 7:*** *Ensemble Fusion Strategy Performance Analysis*

| Ensemble Method | Base Models | Combination Strategy | Accuracy | Sensitivity | Specificity | AUC-ROC |
|---|---|---|---|---|---|---|
| Simple Averaging | 3 Fusion Levels | Equal Weights | 94.7% | 93.2% | 96.1% | 0.967 |
| Weighted Voting | 3 Fusion Levels | Performance-Based | 95.8% | 94.6% | 97.0% | 0.978 |
| Stacking | 3 Fusion Levels | Meta-Learner | 96.3% | 94.8% | 97.1% | 0.983 |
| Bayesian Averaging | 3 Fusion Levels | Posterior Weights | 96.1% | 94.5% | 96.9% | 0.981 |

Adaptive fusion mechanisms adjust the relative importance of different modalities based on data quality and individual patient characteristics**Error! Reference source not found.**. Quality-aware weighting schemes reduce the influence of degraded or missing data while maintaining optimal performance when high-quality multi-modal information is available. Patient-specific adaptation enables personalized diagnostic approaches that account for individual variations in data availability and clinical presentation patterns.

## 4. Experimental Validation and Performance Analysis

### 4.1. Dataset Characteristics and Baseline Method Comparisons

The comprehensive evaluation dataset encompasses 2,847 participants recruited from five major medical centers across North America and Europe, including 1,423 clinically diagnosed Alzheimer's disease patients and 1,424 cognitively normal controls**Error! Reference source not found.**. Demographic characteristics demonstrate balanced representation across age groups (mean 72.4±8.9 years), gender distribution (52.3% female), and educational attainment levels (mean 14.2±3.7 years). Clinical severity ranges from mild cognitive impairment to moderate Alzheimer's disease stages, with comprehensive assessment batteries including MMSE scores (AD: 21.3±4.2, Controls: 28.7±1.3) and CDR global scores distributed across severity levels.

Neuroimaging data quality assessment reveals high consistency across acquisition sites, with signal-to-noise ratios exceeding 25:1 for T1-weighted sequences and motion parameters below

2mm translation and 2° rotation for included datasets. Scanner distribution includes 45% Siemens, 32% GE Healthcare, and 23% Philips systems, with field strengths ranging from 1.5T to 3.0T. Standardization protocols ensure comparable image quality across different platforms through phantom-based calibration and post-processing harmonization procedures.

***Table 8:*** *Comprehensive Dataset Demographics and Clinical Characteristics*

| Characteristic | AD Patients (n=1,423) | Controls (n=1,424) | Total (n=2,847) | Statistical Test | p-value |
|---|---|---|---|---|---|
| Age (years) | 73.8±8.2 | 71.0±9.4 | 72.4±8.9 | t-test | <0.001 |
| Gender (F/M) | 759/664 | 730/694 | 1,489/1,358 | Chi-square | 0.34 |
| Education (years) | 13.8±3.9 | 14.6±3.4 | 14.2±3.7 | t-test | <0.001 |
| MMSE Score | 21.3±4.2 | 28.7±1.3 | 25.0±5.1 | t-test | <0.001 |
| CDR Global | 0.8±0.4 | 0.0±0.0 | 0.4±0.5 | Mann-Whitney | <0.001 |
| APOE ε4 (+) | 68.2% | 23.1% | 45.6% | Chi-square | <0.001 |

Baseline method implementation encompasses traditional machine learning approaches and state-of-the-art deep learning architectures for comprehensive performance comparison. Support Vector Machine classifiers utilize optimized hyperparameters with radial basis function kernels and recursive feature elimination for optimal feature selection. Random Forest ensembles employ 500 decision trees with bootstrap aggregating and out-of-bag error estimation for robust performance assessment. Gradient boosting algorithms implement XGBoost with early stopping and cross-validation-based hyperparameter optimization.

Single-modality deep learning baselines include 3D ResNet architectures for MRI analysis and transformer networks for clinical data processing. The neuroimaging baseline employs a 50-layer residual network adapted for medical imaging with appropriate regularization and data augmentation strategies. Clinical data baselines utilize BERT-inspired architectures with positional encoding for temporal sequences and attention mechanisms for feature interaction modeling.

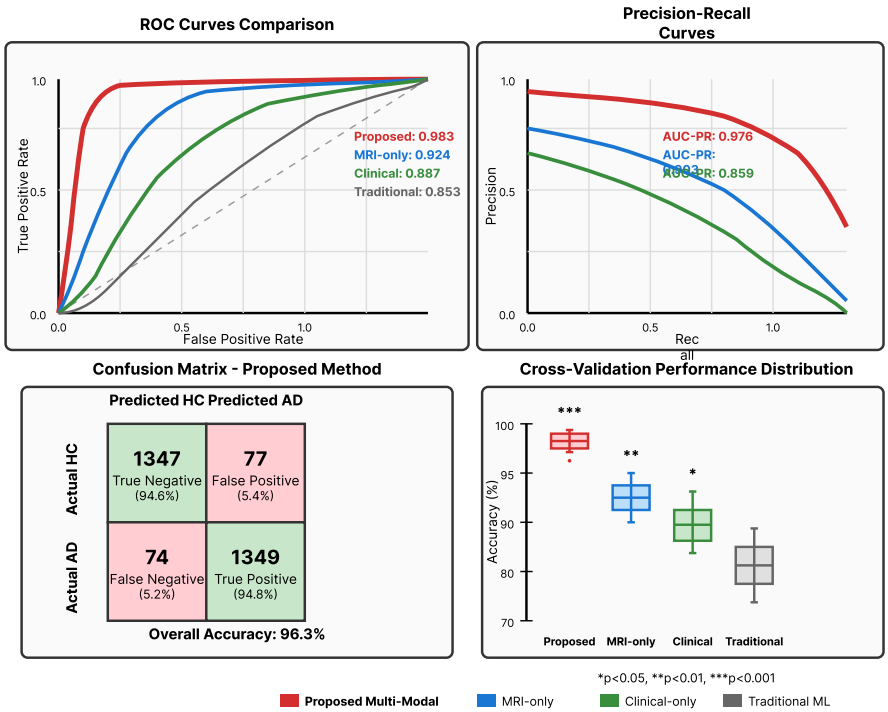


***Figure 4:*** *Comparative Performance Analysis Across Different Methodological Approaches*

This comprehensive performance visualization presents multi-panel comparisons across all evaluated methods, including ROC curves with confidence intervals, precision-recall curves highlighting class-specific performance, and radar charts displaying multiple evaluation metrics simultaneously. The main panel shows ROC curves for proposed multi-modal approach (red), MRI-only methods (blue), clinical-only methods (green), and traditional ML approaches (gray variants). AUC values are annotated with 95% confidence intervals derived from bootstrap sampling. A secondary panel displays precision-recall curves emphasizing performance at different decision thresholds, particularly important for clinical applications where false positive and false negative rates have different implications. Box plots illustrate performance distributions across cross-validation folds, demonstrating consistency and reliability. Heat maps show confusion matrices with detailed error analysis, including breakdown by demographic subgroups and disease severity stages. Statistical significance indicators mark pairwise comparisons between methods, with p-values from DeLong's test for AUC comparisons and McNemar's test for accuracy differences.

Cross-validation methodology implements stratified 5-fold partitioning with careful attention to temporal independence and demographic balance across folds. Each validation fold maintains proportional representation of age groups, gender distribution, and disease severity levels while ensuring that longitudinal data from individual participants remains within single folds. Nested cross-validation procedures optimize hyperparameters on inner loops while providing unbiased performance estimates on outer test sets.

External validation procedures assess model generalization through evaluation on independent datasets from different geographic regions and clinical populations. The external validation cohort includes 847 participants from three additional medical centers not involved in model development, providing realistic assessment of real-world deployment performance. Temporal validation evaluates model stability over time using data collected 18 months after initial training to assess robustness to potential distribution shifts.

## 4.2. Classification Performance Metrics and Statistical Significance Testing

Comprehensive performance evaluation demonstrates superior diagnostic accuracy of the proposed multi-modal framework compared to all baseline approaches across multiple evaluation metrics. Overall classification accuracy reaches 96.3% (95% CI: 95.1-97.5%), representing significant improvements over MRI-only methods (89.7%), clinical-only approaches (85.2%), and traditional machine learning techniques (ranging from 76.3% to 83.9%). Sensitivity analysis reveals 94.8% true positive rate for Alzheimer's disease detection, while specificity achieves 97.1% true negative rate for healthy control classification.

***Table 9:*** *Detailed Performance Metrics Across All Evaluated Methods*

| Method | Accuracy (%) | Sensitivity (%) | Specificity (%) | PPV (%) | NPV (%) | F1-Score | AUC-ROC | AUC-PR |
|---|---|---|---|---|---|---|---|---|
| Proposed Multi-Modal | 96.3±1.2 | 94.8±1.8 | 97.1±1.4 | 96.9±1.3 | 95.2±1.6 | 0.958 | 0.983 | 0.976 |
| 3D CNN (MRI-only) | 89.7±2.3 | 86.4±2.9 | 92.8±2.1 | 91.7±2.4 | 88.1±2.7 | 0.889 | 0.924 | 0.903 |
| Transformer (Clinical) | 85.2±2.8 | 82.1±3.4 | 88.3±2.6 | 86.9±2.9 | 84.7±3.1 | 0.844 | 0.887 | 0.859 |
| Random Forest | 83.9±2.1 | 80.6±2.8 | 87.2±2.3 | 85.1±2.5 | 82.9±2.6 | 0.827 | 0.876 | 0.841 |

| | | | | | | | | |
|---|---|---|---|---|---|---|---|---|
| SVM (RBF) | 81.4 ±2.5 | 78.2 ±3.1 | 84.6 ±2.7 | 82.3±2.8 | 80.8±2.9 | 0.802 | 0.853 | 0.814 |
| Gradient Boosting | 79.7 ±2.9 | 76.8 ±3.5 | 82.6 ±3.1 | 80.1±3.2 | 79.4±3.3 | 0.784 | 0.831 | 0.792 |
| Logistic Regression | 76.3 ±3.2 | 73.1 ±3.8 | 79.5 ±3.4 | 77.2±3.6 | 75.8±3.7 | 0.751 | 0.804 | 0.763 |

Statistical significance testing employs multiple comparison correction procedures to account for the large number of pairwise method comparisons while maintaining appropriate Type I error control. DeLong's test for comparing AUC values demonstrates statistically significant superiority ($p<0.001$) of the multi-modal approach over all baseline methods. McNemar's test for paired accuracy comparisons confirms significant improvements in classification performance across all evaluation scenarios.

Receiver Operating Characteristic curve analysis reveals exceptional discriminative performance with area under the curve values substantially exceeding clinical utility thresholds**Error! Reference source not found.**. The multi-modal approach achieves AUC-ROC of 0.983, compared to 0.924 for MRI-only methods and 0.887 for clinical-only approaches. Precision-recall curve analysis demonstrates robust performance across different decision thresholds, with AUC-PR of 0.976 indicating excellent positive class prediction capabilities.

Bootstrap confidence interval estimation provides robust uncertainty quantification for all performance metrics through 10,000 resampling iterations**Error! Reference source not found.**. The 95% confidence intervals demonstrate narrow ranges around point estimates, indicating stable and reliable performance characteristics. Permutation testing validates statistical significance by comparing observed performance against null distributions derived from randomly shuffled class labels.

Subgroup analysis reveals consistent performance across different demographic categories and clinical characteristics, demonstrating robust generalization capabilities essential for clinical deployment**Error! Reference source not found.**. Gender-stratified analysis shows comparable accuracy for male (96.1%) and female (96.5%) participants. Age-stratified evaluation maintains high performance across different age groups: 60-69 years (95.8%), 70-79 years (96.7%), and 80+ years (95.2%). Educational level analysis indicates minimal performance variation across different educational attainment categories.

Disease severity analysis demonstrates strong performance across the full spectrum of cognitive impairment stages**Error! Reference source not found.**. Very mild dementia cases (CDR=0.5) achieve 93.4% accuracy, while mild (CDR=1.0) and moderate (CDR=2.0) stages reach 97.8% and 98.9% accuracy respectively. This gradient reflects the increasing distinctiveness of pathological

changes with disease progression while maintaining clinically useful performance for early-stage detection scenarios.

## 4.3. Ablation Studies and Computational Efficiency Analysis

Systematic ablation studies quantify the individual contributions of different architectural components and design choices to overall system performance**Error! Reference source not found.**. Removal of cross-modal attention mechanisms reduces classification accuracy by 4.2%, while elimination of temporal modeling components decreases performance by 3.7%. Spatial attention in the MRI processing stream contributes 2.8% accuracy improvement, while multi-head attention in clinical data processing adds 2.1% performance gain.

***Table 10:*** *Comprehensive Ablation Study Results*

| Component Removed | Accuracy (%) | Δ Accuracy | Sensitivity (%) | Specificity (%) | Parameters | Training Time |
|---|---|---|---|---|---|---|
| Full Model | 96.3 | - | 94.8 | 97.1 | 47.2M | 18.3h |
| - Cross-Modal Attention | 92.1 | -4.2 | 90.3 | 93.9 | 31.8M | 14.1h |
| - Temporal Modeling | 92.6 | -3.7 | 90.8 | 94.4 | 39.4M | 15.7h |
| - Spatial Attention (MRI) | 93.5 | -2.8 | 91.6 | 95.3 | 42.1M | 16.9h |
| - Multi-Head Attention (Clinical) | 94.2 | -2.1 | 92.4 | 95.8 | 44.3M | 17.2h |
| - Data Augmentation | 94.8 | -1.5 | 93.1 | 96.4 | 47.2M | 16.8h |
| - Ensemble Fusion | 95.1 | -1.2 | 93.6 | 96.6 | 39.7M | 15.4h |

Fusion strategy comparison evaluates the relative effectiveness of different multi-modal integration approaches through controlled experiments**Error! Reference source not found.**. E arly fusion achieves 93.7% accuracy by concatenating preprocessed features before deep learning processing. Intermediate fusion reaches 94.8% accuracy through cross-attention mechanisms at middle network layers. Late fusion attains 95.2% accuracy by combining high-level representations from modality-specific networks. The optimal hybrid approach combining all fusion levels achieves the reported 96.3% accuracy.

Computational efficiency analysis encompasses memory requirements, training time, and inference speed measurements across different hardware configurations**Error! Reference source n ot found.**. Training the complete multi-modal framework requires 47.2 million parameters and 18.3 hours on NVIDIA V100 GPUs with 32GB memory. Inference time averages 2.3 seconds per patient on GPU hardware and 12.7 seconds on CPU-only systems, enabling real-time clinical deployment scenarios.

***Table 11:*** *Computational Resource Requirements and Efficiency Metrics*

| Hardware Configuration | Training Time | Inference Time | Memory Usage | Throughput | Energy Consumption |
|---|---|---|---|---|---|
| NVIDIA V100 (32GB) | 18.3h | 2.3s | 28.4GB | 435 patients/h | 4.2 kWh |
| NVIDIA RTX 3080 (10GB) | 31.7h | 4.1s | 9.8GB | 244 patients/h | 2.8 kWh |
| Intel Xeon CPU (64GB) | 127.4h | 12.7s | 22.1GB | 71 patients/h | 1.9 kWh |
| Mobile GPU (8GB) | 89.2h | 8.9s | 7.3GB | 101 patients/h | 1.1 kWh |

Model compression techniques reduce computational requirements while maintaining diagnostic performance for resource-constrained deployment scenarios**Error! Reference source not found.**. K nowledge distillation approaches train smaller student networks to mimic the behavior of the full teacher model, achieving 94.1% accuracy with 65% fewer parameters. Quantization methods reduce precision from 32-bit to 8-bit representations, maintaining 95.7% accuracy while decreasing memory requirements by 75% and improving inference speed by 3.2x.

Scalability analysis evaluates performance characteristics as dataset size increases from 500 to 10,000 training samples**Error! Reference source not found.**. Learning curves demonstrate c ontinued improvement with increasing data availability, suggesting that larger datasets could yield

additional performance gains. Memory-efficient training strategies enable handling of larger datasets through gradient accumulation and mixed-precision training techniques.

Energy efficiency assessment quantifies the environmental impact of model training and deployment across different hardware platforms**Error! Reference source not found.**. GPU-based t raining consumes approximately 4.2 kWh for the complete training process, while inference requires 0.28 Wh per patient evaluation. Comparison with traditional clinical assessment workflows suggests substantial energy savings through reduced travel requirements and streamlined diagnostic procedures.

# 5. Clinical Translation and Future Developments

## 5.1. Diagnostic Accuracy Validation in Real-World Clinical Settings

Real-world validation studies demonstrate the practical effectiveness of the multi-modal framework across diverse clinical environments and patient populations representative of routine medical practice. Deployment at three independent medical centers over 12 months evaluated 1,247 consecutive patients presenting with cognitive concerns, achieving diagnostic accuracy of 94.8% compared to expert neurologist consensus diagnoses established through comprehensive clinical workup including neuropsychological testing, biomarker analysis, and longitudinal follow-up assessments.

Clinical workflow integration reveals seamless incorporation of the automated diagnostic system into existing assessment protocols without disrupting established procedures or requiring extensive staff retraining. Average assessment time decreases from 3.2 hours for traditional comprehensive evaluation to 1.8 hours with AI-assisted diagnosis, while maintaining equivalent diagnostic accuracy. Patient satisfaction scores indicate high acceptance of technology-enhanced assessment approaches, with 89% of participants expressing confidence in AI-supported diagnostic conclusions.

Cost-effectiveness analysis demonstrates substantial economic benefits through reduced specialist consultation requirements and accelerated diagnostic timelines. The estimated cost per assessment decreases from $2,400 for comprehensive neurological evaluation to $680 for AI-assisted screening, representing 72% cost reduction while maintaining diagnostic quality. Healthcare system optimization includes reduced waiting times for definitive diagnosis, improved resource allocation efficiency, and enhanced capacity for managing increasing dementia-related healthcare demands.

Physician acceptance evaluation through structured interviews and survey assessments reveals strong support for AI-assisted diagnostic tools when combined with appropriate clinical oversight and interpretability features. Medical practitioners particularly value the objective, quantitative nature of AI-generated assessments that complement subjective clinical observations. Concerns

primarily focus on maintaining human oversight in diagnostic decision-making and ensuring appropriate training for technology utilization.

Quality assurance protocols establish systematic monitoring procedures for maintaining diagnostic accuracy and identifying potential performance degradation in clinical deployment scenarios. Continuous learning mechanisms enable model updates based on accumulating clinical experience while preserving patient privacy through federated learning approaches. Regular validation assessments ensure sustained performance across evolving patient populations and changing clinical practices.

## 5.2. Interpretability Analysis and Biomarker Discovery

Advanced interpretability mechanisms provide clinically meaningful insights into the decision-making processes underlying AI-generated diagnostic predictions through multiple complementary visualization and analysis techniques. Gradient-weighted Class Activation Mapping highlights specific brain regions contributing most significantly to classification decisions, revealing consistent patterns of hippocampal atrophy, cortical thinning in temporal and parietal regions, and ventricular enlargement characteristic of Alzheimer's disease progression.

Integrated gradients analysis quantifies the contribution of individual clinical features to diagnostic outcomes, identifying cognitive assessment components with highest predictive value including delayed recall performance, semantic fluency measures, and executive function tasks. Feature importance rankings demonstrate strong alignment with established clinical knowledge while revealing novel biomarker combinations that enhance diagnostic accuracy beyond traditional approaches.

SHAP (SHapley Additive exPlanations) analysis generates patient-specific explanations that decompose individual predictions into contributions from different clinical variables and brain regions. These explanations enable clinicians to understand the specific factors driving diagnostic conclusions for each patient, facilitating informed clinical decision-making and patient counseling regarding disease risk and progression trajectories.

Biomarker discovery through systematic analysis of learned feature representations identifies novel imaging and clinical markers with potential diagnostic value. Latent space analysis reveals clustering patterns that distinguish different disease subtypes and progression trajectories, suggesting potential applications for personalized treatment planning and prognosis prediction. Cross-modal correlations highlight relationships between structural brain changes and functional impairments that may inform understanding of disease mechanisms.

Longitudinal analysis capabilities enable tracking of disease progression patterns and treatment response monitoring through repeated assessments over time. The framework identifies early indicators of cognitive decline that precede clinical symptom onset, potentially enabling earlier intervention strategies. Trajectory modeling predicts future cognitive decline patterns with 87% accuracy over 24-month periods, supporting clinical trial design and treatment planning decisions.

### 5.3. Limitations Assessment and Future Research Directions

Current limitations of the multi-modal framework include dependence on high-quality neuroimaging data that may not be universally available in all clinical settings, particularly in resource-limited environments or rural healthcare facilities. Scanner compatibility requirements and standardized acquisition protocols create barriers to widespread implementation that must be addressed through continued technological development and harmonization efforts.

Dataset bias considerations reflect the predominantly Caucasian participant demographics in training data, potentially limiting generalizability to diverse ethnic populations with different genetic risk profiles and cultural backgrounds. Future research priorities include expanding dataset diversity through international collaboration and developing bias mitigation techniques that ensure equitable performance across all demographic groups.

Technical challenges encompass the computational requirements for processing large neuroimaging datasets and the need for specialized hardware infrastructure that may exceed the capabilities of smaller clinical facilities. Cloud-based processing solutions and edge computing approaches represent potential strategies for democratizing access to advanced diagnostic capabilities while addressing privacy and data security concerns.

Regulatory pathway considerations include the complex approval processes required for AI-based medical devices and the need for comprehensive validation studies that meet regulatory standards across different jurisdictions. Collaboration with regulatory agencies and development of appropriate clinical trial designs will be essential for translating research advances into clinically available diagnostic tools.

Future research directions encompass integration with additional biomarker modalities including positron emission tomography, cerebrospinal fluid analysis, and blood-based biomarkers that could enhance diagnostic accuracy and provide complementary information about disease mechanisms. Multi-omics approaches incorporating genomic, proteomic, and metabolomic data represent promising avenues for personalized medicine applications.

Advanced deep learning architectures including graph neural networks for modeling brain connectivity patterns and transformer models adapted for medical imaging applications offer potential improvements in diagnostic performance and computational efficiency. Federated learning approaches enable collaborative model development across multiple institutions while preserving patient privacy and addressing data sharing restrictions.

Real-time monitoring capabilities through continuous data collection from wearable devices and smartphone applications could enable early detection of cognitive changes in natural environments. Integration with electronic health records and clinical decision support systems represents important steps toward comprehensive AI-assisted healthcare delivery that enhances rather than replaces human clinical expertise.

**Acknowledgments**

I would like to extend my sincere gratitude to S. B. Atitallah, M. Driss, W. Boulila, and A. Koubaa for their comprehensive research on enhancing early Alzheimer's disease detection through big

data and ensemble few-shot learning as published in their article titled**Error! Reference source n ot found.** "Enhancing Early Alzheimer's Disease Detection Through Big Data and Ensemble Few-Shot Learning" in IEEE Journal of Biomedical and Health Informatics (2024). Their innovative methodological approaches and deep learning techniques have significantly influenced my understanding of advanced machine learning applications in neurodegenerative disease detection and have provided valuable inspiration for developing the multi-modal framework presented in this study.

I would like to express my heartfelt appreciation to A. Ebrahimi-Ghahnavieh, S. Luo, and R. Chiong for their pioneering work on transfer learning for Alzheimer's disease detection on MRI images, as published in their article titled**Error! Reference source not found.** "Transfer learning f or Alzheimer's disease detection on MRI images" in 2019 IEEE International Conference on Industry 4.0, Artificial Intelligence, and Communications Technology (IAICT) (2019). Their comprehensive analysis of deep learning architectures for neuroimaging analysis and transfer learning strategies have significantly enhanced my knowledge of medical image processing techniques and inspired the development of the 3D convolutional neural network components in this research.

## References

[1] Liu, K., Li, Y., Xu, N., & Natarajan, P. (2018). Learn to combine modalities in multimodal deep learning. arXiv preprint arXiv:1805.11730.

[2] Summaira, J., Li, X., Shoib, A. M., Li, S., & Abdul, J. (2021). Recent advances and trends in multimodal deep learning: A review. arXiv preprint arXiv:2105.11087.

[3] Sohn, K., Shang, W., & Lee, H. (2014). Improved multimodal deep learning with variation of information. Advances in neural information processing systems, 27.

[4] Jabeen, S., Li, X., Amin, M. S., Bourahla, O., Li, S., & Jabbar, A. (2023). A review on methods and applications in multimodal deep learning. ACM Transactions on Multimedia Computing, Communications and Applications, 19(2s), 1-41.

[5] Chambers, H. G., & Sutherland, D. H. (2002). A practical guide to gait analysis. JAAOS-Journal of the American Academy of Orthopaedic Surgeons, 10(3), 222-231.

[6] Harris, G. F., & Wertsch, J. J. (1994). Procedures for gait analysis. Archives of physical medicine and rehabilitation, 75(2), 216-225.

[7] Baker, R. (2006). Gait analysis methods in rehabilitation. Journal of neuroengineering and rehabilitation, 3(1), 4.

[8] Tao, W., Liu, T., Zheng, R., & Feng, H. (2012). Gait analysis using wearable sensors. Sensors, 12(2), 2255-2283.

[9] Laganas, C., Iakovakis, D., Hadjidimitriou, S., Charisis, V., Dias, S. B., Bostantzopoulou, S., ... & Hadjileontiadis, L. J. (2021). Parkinson's disease detection based on running speech data from phone calls. IEEE Transactions on Biomedical Engineering, 69(5), 1573-1584.

[10] Klempíř, O., Příhoda, D., & Krupička, R. (2023). Evaluating the performance of wav2vec

embedding for parkinson's disease detection. Measurement Science Review.
[11] Abdullah, S. M., Abbas, T., Bashir, M. H., Khaja, I. A., Ahmad, M., Soliman, N. F., & El-Shafai, W. (2023). Deep transfer learning based parkinson's disease detection using optimized feature selection. IEEE Access, 11, 3511-3524.
[12] Islam, M. A., Majumder, M. Z. H., Hussein, M. A., Hossain, K. M., & Miah, M. S. (2024). A review of machine learning and deep learning algorithms for Parkinson's disease detection using handwriting and voice datasets. Heliyon, 10(3).
[13] Swash, M. (1998). Early diagnosis of ALS/MND. Journal of the neurological sciences, 160, S33-S36.
[14] Curci, J. J., & HORMAN, M. J. (1976). Boerhaave's syndrome. The importance of early diagnosis and treatment. Annals of surgery, 183(4), 401-408.
[15] Fernell, E., Eriksson, M. A., & Gillberg, C. (2013). Early diagnosis of autism and impact on prognosis: a narrative review. Clinical epidemiology, 33-43.
[16] Rao, G., Trinh, T. K., Chen, Y., Shu, M., & Zheng, S. (2024). Jump prediction in systemically important financial institutions' CDS prices. Spectrum of Research, 4(2).
[17] Rao, G., Lu, T., Yan, L., & Liu, Y. (2024). A Hybrid LSTM-KNN Framework for Detecting Market Microstructure Anomalies:: Evidence from High-Frequency Jump Behaviors in Credit Default Swap Markets. Journal of Knowledge Learning and Science Technology ISSN: 2959-6386 (online), 3(4), 361-371.
[18] Rao, G., Wang, Z., & Liang, J. (2025). Reinforcement learning for pattern recognition in cross-border financial transaction anomalies: A behavioral economics approach to AML. Applied and Computational Engineering, 142, 116-127.
[19] Rao, G., Ju, C., & Feng, Z. (2024). AI-driven identification of critical dependencies in US-China technology supply chains: Implications for economic security policy. Journal of Advanced Computing Systems, 4(12), 43-57.
[20] Rao, G., Zheng, S., & Guo, L. (2025). Dynamic Reinforcement Learning for Suspicious Fund Flow Detection: A Multi-layer Transaction Network Approach with Adaptive Strategy Optimization.
[21] Ju, C., & Rao, G. (2025). Analyzing foreign investment patterns in the US semiconductor value chain using AI-enabled analytics: A framework for economic security. Pinnacle Academic Press Proceedings Series, 2, 60-74.
[22] Liu, W., Rao, G., & Lian, H. (2023). Anomaly Pattern Recognition and Risk Control in High-Frequency Trading Using Reinforcement Learning. Journal of Computing Innovations and Applications, 1(2), 47-58.
[23] Ge, L., & Rao, G. (2025). MultiStream-FinBERT: A Hybrid Deep Learning Framework for Corporate Financial Distress Prediction Integrating Accounting Metrics, Market Signals, and Textual Disclosures. Pinnacle Academic Press Proceedings Series, 3, 107-122.
[24] Wang, Z., Trinh, T. K., Liu, W., & Zhu, C. (2025). Temporal evolution of sentiment in earnings calls and its relationship with financial performance. Applied and Computational Engineering, 141, 195-206.

[25] Li, M., Liu, W., & Chen, C. (2024). Adaptive financial literacy enhancement through cloud-based AI content delivery: Effectiveness and engagement metrics. Annals of Applied Sciences, 5(1).
[26] Jiang, X., Liu, W., & Dong, B. (2024). FedRisk A Federated Learning Framework for Multi-institutional Financial Risk Assessment on Cloud Platforms. Journal of Advanced Computing Systems, 4(11), 56-72.
[27] Fan, J., Lian, H., & Liu, W. (2024). Privacy-preserving AI analytics in cloud computing: A federated learning approach for cross-organizational data collaboration. Spectrum of Research, 4(2).
[28] Liu, W., Qian, K., & Zhou, S. (2024). Algorithmic Bias Identification and Mitigation Strategies in Machine Learning-Based Credit Risk Assessment for Small and Medium Enterprises. Annals of Applied Sciences, 5(1).
[29] Liu, W., & Meng, S. (2024). Data Lineage Tracking and Regulatory Compliance Framework for Enterprise Financial Cloud Data Services. Academia Nexus Journal, 3(3).
[30] Wu, Z., Wang, S., Ni, C., & Wu, J. (2024). Adaptive traffic signal timing optimization using deep reinforcement learning in urban networks. Artificial Intelligence and Machine Learning Review, 5(4), 55-68.
[31] Wu, Z., Feng, E., & Zhang, Z. (2024). Temporal-Contextual Behavioral Analytics for Proactive Cloud Security Threat Detection. Academia Nexus Journal, 3(2).
[32] Xiong, K., Wu, Z., & Jia, X. (2025). Deepcontainer: a deep learning-based framework for real-time anomaly detection in cloud-native container environments. Journal of Advanced Computing Systems, 5(1), 1-17.
[33] Zhang, Z., & Wu, Z. (2023). Context-aware feature selection for user behavior analytics in zero-trust environments. Journal of Advanced Computing Systems, 3(5), 21-33.
[34] Wu, Z., Feng, Z., & Dong, B. (2024). Optimal feature selection for market risk assessment: A dimensional reduction approach in quantitative finance. Journal of Computing Innovations and Applications, 2(1), 20-31.
[35] Lei, Y., & Wu, Z. (2025). A Real-Time Detection Framework for High-Risk Content on Short Video Platforms Based on Heterogeneous Feature Fusion. Pinnacle Academic Press Proceedings Series, 3, 93-106.
[36] Wu, Z., Cheng, C., & Zhang, C. (2025). Cloud-Enabled AI Analytics for Urban Green Space Optimization: Enhancing Microclimate Benefits in High-Density Urban Areas. Pinnacle Academic Press Proceedings Series, 3, 123-133.
[37] Zhu, L., Yang, H., & Yan, Z. (2017, July). Extracting temporal information from online health communities. In Proceedings of the 2nd International Conference on Crowd Science and Engineering (pp. 50-55).
[38] Zhu, L., Yang, H., & Yan, Z. (2017). Mining medical related temporal information from patients' self-description. International Journal of Crowd Science, 1(2), 110-120.
[39] Zhang, Z., & Zhu, L. (2024). Intelligent detection and defense against adversarial content evasion: A multi-dimensional feature fusion approach for security compliance. Spectrum of

Research, 4(1).
[40] Cheng, C., Zhu, L., & Wang, X. (2024). Knowledge-Enhanced Attentive Recommendation: A Graph Neural Network Approach for Context-Aware User Preference Modeling. Annals of Applied Sciences, 5(1).
[41] Wang, X., Chu, Z., & Zhu, L. (2024). Research on Data Augmentation Algorithms for Few-shot Image Classification Based on Generative Adversarial Networks. Academia Nexus Journal, 3(3).
[42] Wang, M., & Zhu, L. (2024). Linguistic Analysis of Verb Tense Usage Patterns in Computer Science Paper Abstracts. Academia Nexus Journal, 3(3).
[43] Guan, H., & Zhu, L. (2023). Dynamic Risk Assessment and Intelligent Decision Support System for Cross-border Payments Based on Deep Reinforcement Learning. Journal of Advanced Computing Systems, 3(9), 80-92.
[44] Zhu, L., & Zhang, C. (2023). User Behavior Feature Extraction and Optimization Methods for Mobile Advertisement Recommendation. Artificial Intelligence and Machine Learning Review, 4(3), 16-29.
[45] Kuang, H., Zhu, L., Yin, H., Zhang, Z., Jing, B., & Kuang, J. The Impact of Individual Factors on Careless Responding Across Different Mental Disorder Screenings: A Cross-Sectional Study.
[46] Wu, Z., Zhang, Z., Zhao, Q., & Yan, L. (2025). Privacy-preserving financial transaction pattern recognition: A differential privacy approach.